

Bistable behavior of silicon atoms in the (110) surface of gallium arsenide

J. K. Garleff, A. P. Wijnheijmer, C. N. v. d. Enden, and P. M. Koenraad*

*COBRA Inter-University Research Institute, Department of Applied Physics, Eindhoven University of Technology,
P. O. Box 513, NL-5600 MB Eindhoven, The Netherlands*

(Received 17 February 2011; published 11 August 2011)

Reversibly switching between the hydrogenic substitutional donor configuration and a previously unknown negatively charged interstitial configuration of silicon (Si) impurities in the surface layer of gallium arsenide (GaAs) was observed. The unexpected negatively charged state of Si_{Ga} stresses that the surface dominates the properties of dopant atoms close to it. We find that the negatively charged state is favorable in the case of the bare surface, whereas the donor configuration is only favorable with the tip of the scanning tunneling microscope (STM) nearby. The Si atom randomly switches between both bistable configurations. The bistable behavior was characterized with STM as a function of the applied voltage, the tunneling current, the temperature, and the local environment. The voltage dependence suggests a similar potential landscape as derived for DX^- centers in bulk GaAs. Increased switching rates at higher currents point on an inelastic process, although with a rather low efficiency. The switching rate is constant below 20 K, whereas it increases above 20 K. This indicates a nonthermal process below 20 K, probably elastic excitations in combination with quantum tunneling, whereas the switching is thermally activated at higher temperatures.

DOI: [10.1103/PhysRevB.84.075459](https://doi.org/10.1103/PhysRevB.84.075459)

PACS number(s): 73.20.Hb, 68.37.Ef, 66.35.+a

I. INTRODUCTION

Impurities in semiconductors are investigated for a variety of reasons, such as doping of the material to tailor electronic devices. In contrast to the well established research on bulk dopants, defects in semiconductor surfaces started to play a role only recently in the development of nanowire sensors.¹ Other studies characterizing surface defects aimed for fundamental science. A review on defects studied with STM and related techniques was given by Ebert.² A broad variety of dopants has been studied below the GaAs(110) surface: beryllium, carbon, and zinc as shallow acceptors,^{3–6} manganese as a deep acceptor,^{7,8} and Si as a shallow donor^{9–11} and a shallow acceptor.^{12,13} In most cases the impurity atoms are described by their bulk-like properties. Typically the surface is taken into account by assuming only minor modifications, despite significant surface induced changes can occur. For example, we recently reported a broken symmetry of acceptor wave functions¹⁴ and an enhanced binding energy for Si donors and Mn acceptors^{15,16} close to the GaAs(110) surface. The latter was also predicted by tight binding calculations.¹⁷

In this paper we present evidence for a nonthermal process, most likely inelastic excitations, possibly in combination with quantum tunneling, involved in a bistable behavior of Si atoms in the top layer of GaAs(110). The Si atom switches between two bistable bond configurations in the semiconductor crystal. This is a unique model system, because we measure *on* the GaAs(110) surface but see the Si atoms moving *in* the highly ordered binding situation of a semiconductor lattice. The switch between the two configurations is abrupt, although the time between two switching events is long, on the order of seconds to minutes. We investigate several dependencies, and provide arguments that more than electrostatics is involved, most likely a lattice relaxation of the Si atom.

Figure 1 summarizes this behavior. The STM image in Fig. 1(b) shows a surface Si atom, imaged at a low positive sample voltage of 0.5 V and 0.5 nA. The fast scan direction is

from right to left, and the slow scan direction is from top to bottom. The Si atom has two distinct appearances: It is either dark or bright with an ionization disk. We interpret the white state as a substitutional donor configuration [Fig. 1(a)], and the dark state as an interstitial-like configuration [Fig. 1(c)], which will be substantiated later. Two bistable configurations suggest a potential landscape with two minima, separated by an energy barrier E_{barr} [Fig. 1(d)]. Figure 1(e) shows the switching rate τ^{-1} versus temperature T between 5 and 20 K. τ^{-1} is constant below 20 K, suggesting a nonthermal behavior, whereas it increases with T above 20 K, suggesting a thermally excited process. In the next sections we elaborate the experimental results, and discuss the possible models. The previously unknown negatively charged state of the Si atom and its bistable behavior in the surface of GaAs stress the particular properties of dopant atoms that are embedded close to a surface.

II. EXPERIMENTAL RESULTS

Our STM measurements were performed on the {110} cleavage surface of Si-doped GaAs. The Omicron LT-STM and the preparation of the tungsten tips have been described elsewhere.^{15,18} We cleaved the samples in ultrahigh vacuum from commercially available Si-doped GaAs wafers with an average doping level of $\sim 10^{18} \text{ cm}^{-3}$. The observations presented here were similarly measured on samples with a lower Si doping concentration of $\sim 10^{17} \text{ cm}^{-3}$. We present the results measured on the highly doped material because it allows better statistics.

We identified the Si donors in our measurements according to their well known contrast.¹¹ The depth of the donors below the surface was determined based on the topographic height contrast, which is assumed to decrease monotonically with the depth of the donor below the surface.^{9,19} Taking into account that the contrast of Si donors in odd layers (1,3,5,...) is centered at a Ga site of the surface lattice, whereas it is centered

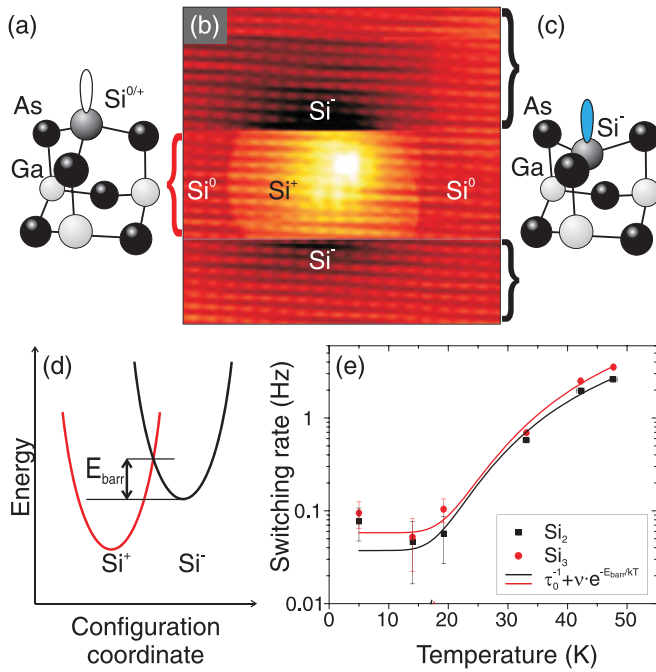


FIG. 1. (Color online) Switching of a Si atom in the GaAs(110) surface between the substitutional donor Si^+ with (a) an empty dangling bond and (c) the negatively charged interstitial Si^- with a filled dangling bond. (b) STM topograph at the critical voltage shows both configurations. The slow scanning direction is parallel to the horizontal axis. (d) Schematic potential landscape of the bistable system. (e) Switching rate versus temperature at 25 pA.

around an As site for Si donors substituted in an even layer (2,4,6, ...), Si donors in the first few layers were identified with layer-by-layer precision. Note that we count the surface layer as 1. An example is shown in Fig. 2, where the inset shows the high and low frequency parts of a topographic cross section. This measurement is obtained at -2.5 V, where the As sublattice is imaged. The maximum of the envelope coincides with a minimum in the atomic corrugation, thus the maximum coincides with a Ga atom, and therefore this donor is located in an odd layer.

All Si atoms in the surface layer show a bistable contrast: They resemble Si_{Ga} donors at voltages far from 0 V, but turn into negatively charged defects at low positive voltage. STM and scanning tunneling spectroscopy (STS) at voltages far from 0 V identified the donor configuration as a substitutional Si atom in the surface layer of GaAs(110). Minor differences of the surface layer Si impurity to donors that are buried more deeply below the GaAs(110) surface have been reported.⁹ They were ascribed to the specific binding conditions in the first layer of the surface.²⁰

The topography measurements obtained at 5 K shown in Figs. 3(a) to 3(c) for different sample voltages give an overview of the Si induced features in GaAs. At high positive bias voltages we observe bright protrusions with and without a circular sharp edge, and dark depressions. The bright features are identified as positively ionized donors,^{2,10,11} where the donor is ionized inside the circular edge, and neutral outside.^{15,21} The dark features are assigned to Si atoms substituted on an As site, which act as acceptors. As expected

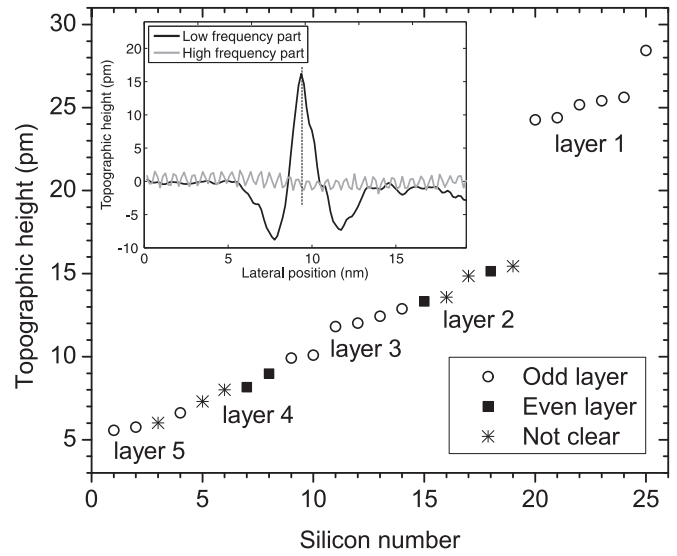


FIG. 2. Topographic height contrast of individual Si atoms. The inset shows a cross section through a donor, measured at -2.5 V. The low frequency part shows the Friedel oscillation, and the high frequency part shows the atomic corrugation. The maximum of the envelope coincides with a minimum in the atomic corrugation, corresponding to a donor in an even layer. We count the surface layer as 1.

for a highly doped sample,^{2,12,13} $\sim 20\%$ of the Si atoms were incorporated as Si_{As} acceptors.

Figure 4 shows examples of both types of subsurface impurities; a Si_{As} acceptor is labeled A^- , a Si_{Ga} donor is labeled D^+ . Si_{Ga} impurities that are embedded in the surface

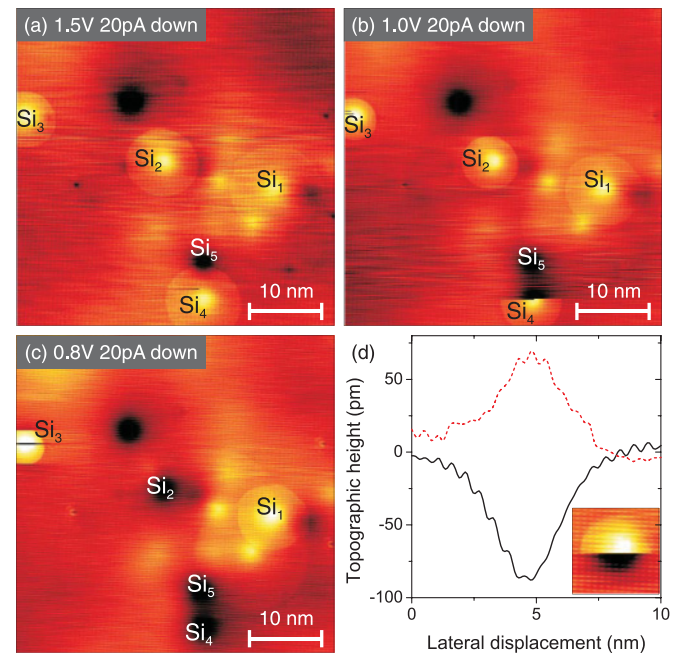


FIG. 3. (Color online) (a)–(c) STM topographs of Si-doped GaAs(110) measured at 5 K and 20 pA. The applied voltage is given in the image. Up and down refers to the slow scanning direction. Si_1 and Si_2 show the normal donor contrast, Si_3 and Si_4 switch to a black contrast at low voltage, and Si_5 is an acceptor, Si_{As} . (d) Shows cross sections before (black line) and after (red dotted line) switching a Si atom from Si^- to Si^+ .

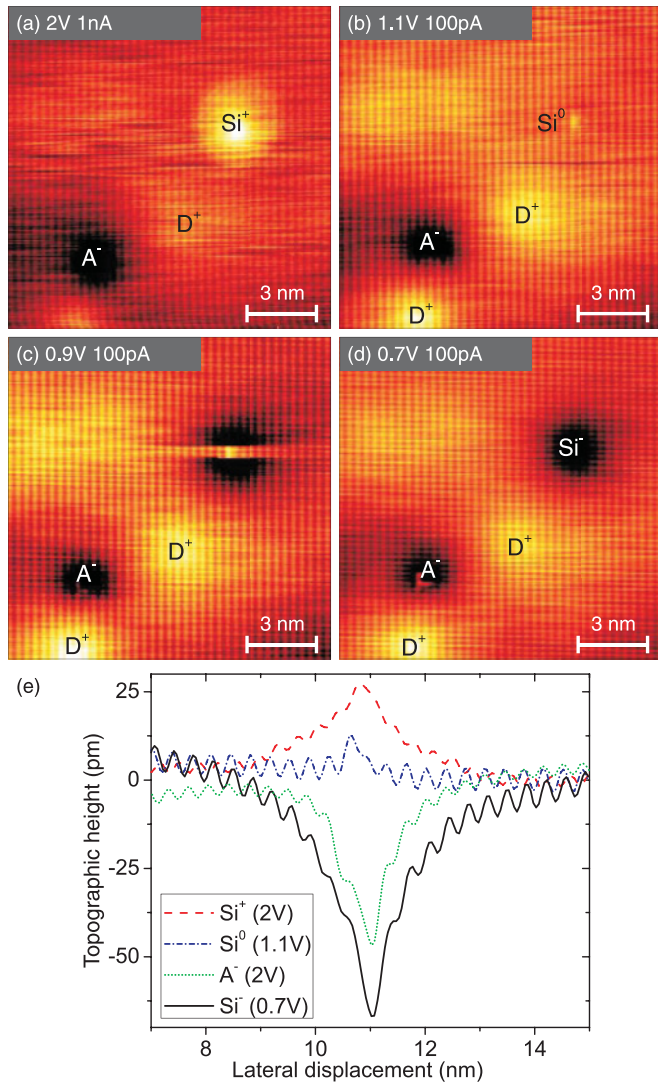


FIG. 4. (Color online) (a)–(d) Topography images at different voltages showing an ionized subsurface donor D^+ and a subsurface acceptor A^- . The surface Si atom can have three charge states: (a) positively ionized Si^+ , (b) neutral Si^0 , and (c) negatively charged Si^- . (e) Cross sections through the defects.

layer switch in a bistable manner between a white and black configuration. The subsequent images Figs. 4(a) to 4(d) show the three possible charge states of this impurity. Figure 4(a) shows the positively ionized surface donor Si^+ at a sample voltage of 2 V, and Fig. 4(b) shows the neutral surface donor Si^0 at a sample voltage of 1.1 V. At a critical voltage $V_{crit} = 0.9$ V [Fig. 4(c)], the Si_{Ga} in the surface switches between the donor and a deep-trap-like configuration at random positions. At a sample voltage of 0.7 V $< V_{crit}$, shown in Fig. 4(d), the Si_{Ga} in the surface is found in the negatively charged Si^- configuration. The charge states of the different configurations Si^+ , Si^0 , and Si^- , are demonstrated by the line profiles along the [001] direction (horizontal axis) in Fig. 4(e). The red dashed line depicts the cross section through the ionized Si^+ , the blue dash-dotted line through the neutral Si^0 , and the black solid line through the negatively charged Si^- configuration of the Si_{Ga} in the surface. The green dotted line profile through the negatively charged Si_{As} acceptor A^- reflects the shape of

the Coulomb potential. Comparing the contrasts of the Si^- defect with the defects that carry a single negative charge, A^- , or a single positive charge, Si^+ , we see that the Si^- contrast resembles the A^- contrast, although the amplitude of the topographic contrast is different. The amplitudes differ from each other, because the line sections plotted in Fig. 4(e) reflect impurities in different depths, that are furthermore measured at different voltages. In Fig. 3(d) we compare line sections before and after the switching event. The black line depicts the negatively charged Si^- , the red dashed line depicts the ionized donor Si^+ . Both lines show the profile of a Coulomb potential with the same amplitude (within 20%). From the inverted contrast we conclude that Si^- carries one negative elementary charge.

In the previous paragraph, we distinguished three charge states, even though we identified only two configurations. The reason is that the donor configuration has two possible charge states. We thus identify two mechanisms that can charge the charge state: ionization and switching. The ionization is a fast ($\ll 1$ ms), purely electrostatic process.^{15,21} The second manipulation—switching—involves a change in the configuration, and is a much slower process where seconds to minutes are involved. The surface Si atoms switch between a donor configuration (where ionization is observed from Si^0 to Si^+) and a negatively charged configuration Si^- . Moreover, in Ref. 22 we showed that a second electron can be bound to donors close to the surface, including Si atoms in the surface layer that are in the donor configuration. In this case, the Si atom is also negatively charged, but its configuration is qualitatively different than the dark state discussed in the current work. The second electron in the negatively charged donor configuration (second ring, see Ref. 22) fits to the hydrogenic description of the Si_{Ga} donor, and extends over a few nanometer. Contrarily, the negative charge in the dark configuration discussed in this work, is localized on the Si atom, probably on its dangling bond. Such a strongly localized charge redistribution is expected to affect the bond configuration, and thus likely to induce a lattice relaxation.

Bistable switching suggests a model with two minima separated by a barrier in configuration space. Such a potential landscape is schematically plotted in Fig. 1(e). The parabolas shift with respect to each other when the conditions such as the external voltage are varied. We explored three manners to cross the barrier: By an inelastic process driven by the tunneling current, by thermally activated hopping, and by quantum tunneling. Therefore we investigated the dependence of switching on the tunneling current I_T and the temperature T .

First we address the dependence of the switching on the current setpoint. The I_T dependent measurements depicted in Fig. 5 are conducted with the same tip on the same ensemble of donors as the voltage dependent investigation shown in Fig. 3, and yield the same V_{crit} . Varying I_T clearly affects the time scale of the switching. We define τ^{-1} as the number of switching events per second. At a low current of 20 pA, shown in Fig. 5(a), the donor switches only once during the measurement. At a ten times higher current of 0.2 nA [Fig. 6(b)], the donor switches a few times. This corresponds to 0.071 Hz $< \tau_{0.2nA}^{-1} < 1$ Hz. At a current of 2 nA, the switching rate increases even more: 0.25 Hz $< \tau_{2nA}^{-1} < 4$ Hz. Due to the high switching rate, the Si atom switches in almost every line

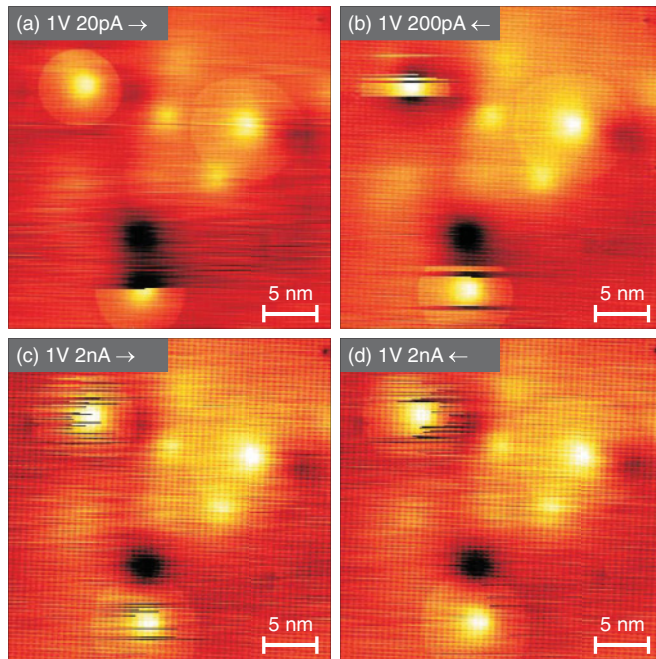


FIG. 5. (Color online) Current dependent topography images of the switching Si impurities from Fig. 3. The time scale of the switching is large at low I_T (a, b), and decreases at higher I_T (c, d). The fast scanning direction is parallel to the horizontal axis, and the direction is indicated by the arrows.

resulting in the rather ragged image at the donor. Note the difference between the forward and the backward scan shown in Figs. 5(c) and 5(d). In both cases the Si atom starts negatively charged and switches to the donor configuration during the scan line. This proves that the negatively charged configuration is favorable in the undisturbed situation when the Si atom is not affected by the tip, whereas the donor configuration is favorable only with the tip nearby. For a more quantitative analysis, we compare the switching rates at 25 and at 250 pA. Averaging all data in the low temperature regime below

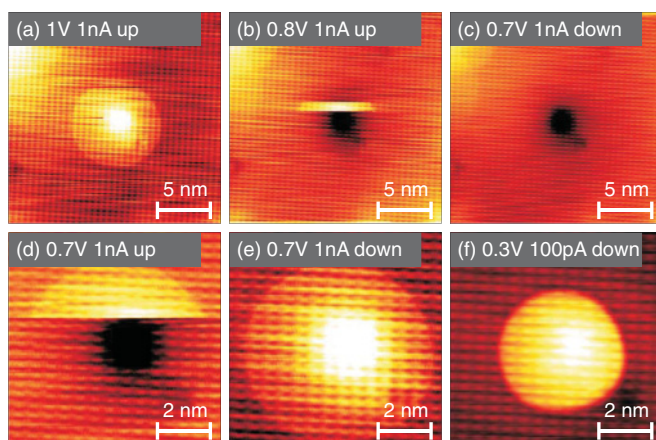


FIG. 6. (Color online) Topography images of a Si atom in the first layer of GaAs(110) at 5 K. (a)–(c) Scanning large frames it switches from white to black as V drops below V_{crit} . (d)–(f) At small scan sizes it stays white even far below V_{crit} . Images are plotted in the original frame size. Up and down refers to the slow scanning direction.

20 K (see next paragraph) yields $\tau_{25\text{ pA}}^{-1} = 0.04 \pm 0.025$ Hz, and $\tau_{250\text{ pA}}^{-1} = 0.45 \pm 0.28$ Hz. The roughly constant ratio $\tau^{-1}/I_T \approx 2.5 \cdot 10^{-10}$ switching events per electron points to an inelastic process. This efficiency is approximately six orders of magnitude smaller than reported for other inelastic processes as scanning tunneling luminescence.²³

A process that is driven by inelastic excitations typically has the highest switching rate when the tip is located on top of the center of the impurity (see, e.g., Ref. 24). This is not the case in our system. The switch from black to white typically does occur with the tip close to the center of the Si atom, but the switch from white to black does not. This happens somewhere in the scan line, when the tip is away from the donor and the distance between tip and impurity is too large to detect the electrostatic effect of the switching event at this position of the tip. However, we observe an enhancement of the switching rate for both transitions. The enhancement in the switching rate for the Si^+ to Si^- transition (white to black) is visible only indirectly. It is evident because the Si atom starts in the black configuration in almost every scan line in Figs. 5(c) and 5(d), whereas it stays white for the rest of the image in Fig. 5(a).

A straightforward way to measure τ^{-1} would be to place the tip on the Si atom, and record the switching events as “random telegraph noise” in the tunneling current. Time traces of the switching motion of atomic pairs on the Pt decorated Ge(001) surface²⁵ were measured this way. When we tried this, no switching occurred at all. To understand this behavior, we varied the frame size as shown in the sequence of images on an individual Si atom in Fig. 6. For large images [Figs. 6(a)–6(c)], the Si atom switches as described above. It is in its white configuration for $V > V_{\text{crit}}$ [Fig. 6(a)], switches during the scan when $V \approx V_{\text{crit}}$ [Fig. 6(b)], and it is in its black configuration for $V < V_{\text{crit}}$. For frame sizes below a threshold of $(9\text{ nm})^2$ [Figs. 6(d)–6(f)], it switches from black to white during the first scan [Fig. 6(d)] and stays white [Fig. 6(e)]. Even when applying a sample voltage far below V_{crit} , the Si atom remains in its white configuration [Fig. 6(f)]. We also tried applying a negative sample voltage down to -0.7 V or retracting the tip >100 nm from the surface for 15 minutes, but the Si atom stayed white. Only after increasing the scan area (i.e., removing the tip laterally), the Si atom turns black again. The critical distance for unpinning was experimentally found on the order of the tip radius. This explains why switching has not been observed in previous STM studies. We use ultrasharp tips with a radius of a few nanometers, whereas in previous STM studies blunter tips were used. We confirmed experimentally that using blunter tips results in the donor to be pinned in the white configuration for large frame size, and switching cannot be observed.

Next we investigate the temperature dependence of the switching dynamics. To investigate purely the influence of the temperature, we need to stay on the same area of the sample and image the same Si atoms. Otherwise different properties of different Si atoms might mask the influence of the temperature. This requires the simultaneous removal of drift while heating up the STM. We succeeded in characterizing the switching behavior of three individual Si atoms as a function of voltage and current for several temperatures between 5 and 50 K in steps of ~ 8 K. Due to the pinning discussed in the

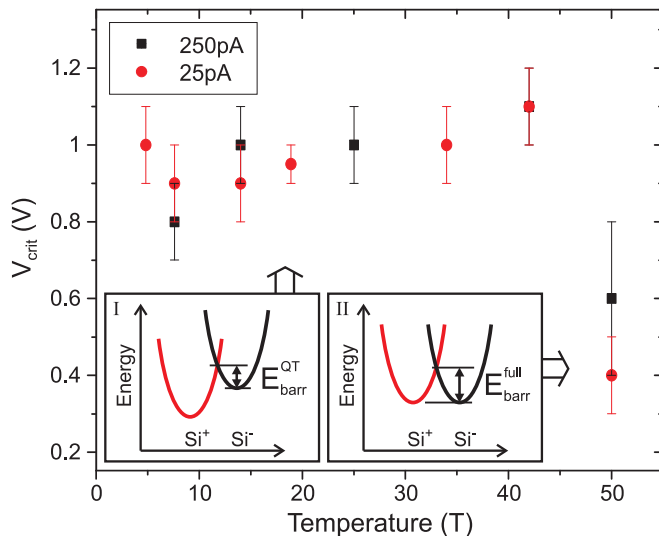


FIG. 7. (Color online) Critical voltage V_{crit} versus temperature.

previous paragraph, we have to measure an image at each temperature, at various voltages and current setpoints, and extract the switching rate from the STM images.

We investigated the dependence on the temperature of both τ^{-1} and V_{crit} . V_{crit} is defined as the voltage where the most switching events occur. We furthermore measure τ^{-1} and V_{crit} at two current setpoints, 25 and 250 pA, because the switching rate depends on I as described above.

The resulting V_{crit} as a function of temperature is plotted in Fig. 7. V_{crit} remains constant for $T < 40$ K, within the uncertainty of the measurement of ~ 100 mV. The critical voltage drastically decreases above ~ 40 K. This trend is confirmed by independent measurements at 77 K, where $V_{\text{crit}} = 0.2$ V was found. Furthermore no significant difference is observed between V_{crit} measured at $I_T = 25$ and 250 pA, which is consistent with the current dependent measurements at 5 K shown in Fig. 5.

Figure 8 shows the experimentally measured switching rates τ^{-1} as a function of temperature and as a function of inverse temperature on a log scale for a current setpoint of 25 and 250 pA. Figures 8(a) and 8(b) show the results for two individual donors at these two setpoints, and Fig. 8(c) shows the result of all three donors together. For temperatures below ~ 20 K we find a constant switching rate, whereas τ^{-1} increases with T above ~ 20 K. We therefore fit the data with the expression for a thermally excited process, with an additional nonthermal (τ_0^{-1}) term²⁶

$$\tau^{-1} = \tau_0^{-1} + \nu \cdot e^{-E_{\text{barr}}/kT}. \quad (1)$$

Here ν corresponds to the attempt frequency and E_{barr} to the energy barrier between the two configurations. The solid lines in Fig. 8 correspond to the fit results. The contribution of the two terms is clear in the plots of τ^{-1} versus the inverse temperature, as is indicated by the dashed lines. The regime where $\log(\tau^{-1})$ decreases linearly with T^{-1} corresponds to the thermally activated term, and the regime where τ^{-1} is constant. This demonstrates the crucial impact of a nonthermal contribution.

TABLE I. Results from fitting $\tau^{-1} = \tau_0^{-1} + \nu \cdot e^{-E_{\text{barr}}/kT}$ to the experimental data of switching rate versus temperature.

	τ_0^{-1} (Hz)	ν (Hz)	E_{barr} (meV)
Si ₁ ^{25pA}	0.02 ± 0.14	206 ± 194	17.03 ± 3.8
Si ₁ ^{250pA}	0.21 ± 0.59	11.0 ± 9.5	5.1 ± 3.4
Si ₂ ^{25pA}	0.037 ± 0.078	59 ± 28	12.8 ± 1.9
Si ₂ ^{250pA}	0.76 ± 0.26	81 ± 141	14.2 ± 7.0
Si ₃ ^{25pA}	0.058 ± 0.082	109 ± 44	14.1 ± 1.6
Si ₃ ^{250pA}	0.39 ± 0.04	22.1 ± 3.5	8.95 ± 0.63
all, 25 pA	0.040 ± 0.085		
all, 250 pA	0.42 ± 0.19		

The parameters τ_0^{-1} , ν and E_{barr} derived from these fits are summarized in Table I. The results are shown separately for the individual Si atoms at both current setpoints. There is a clear dependence of τ_0^{-1} on the current setpoints, and therefore the value averaged over all three donors is given. Such a clear trend does not exist for the other parameters, and therefore we only show the individual results. The resulting barrier height is similar to the barrier extracted for a roughly comparable process studied by Heinrich *et al.*,²⁶ whereas the attempt frequency is low compared to the literature. For example, a frequency in the THz regime is expected for phonons, and the impinging electrons have a frequency of tens of MHz to GHz. Experimentally a frequency of $\sim 10^6$ Hz was observed by Heinrich *et al.*²⁶ for hopping CO molecules on Cu(111), which they could not explain. We observe a frequency of ~ 100 Hz, which is even a few orders of magnitude lower. This suggests that a more complicated mechanism is involved than purely the excitation of phonons. This confirms the above-mentioned concerns about the Si impurity switching while the tip is located at random position, which is not fully expected under the assumption of a simple inelastic process.

As a last experimental observation, we now discuss the random behavior of the switching. Figure 9 shows subsequent images scanning up and down on a site containing a Si donor in the surface. The position where the Si atom switches, and the exact number of switching events are random. The reason is that the switching takes place on a similar time scale as the time needed to scan one frame. This holds especially for the low T and low I_T regime.

Prior to further interpretation, we briefly summarize the experimental results. The charge states—Si⁻ for the black state and Si⁺ for the white state—are derived from topography images, where both configurations show a Coulombic contrast, but inverted with respect to each other. The black configuration is favorable on the bare surface when the Si atom is not influenced by the tip, and the white state is favorable with the tip close to the Si atom. The time scale is much larger than the time scale involved in the ionization process, which proves that more is involved than purely charging and discharging of the Si atom. The critical voltage, which determines whether the positive or the negative charge state of the Si impurity is found, indicates that electrostatics play a crucial role for the underlying potential landscape. The dependence

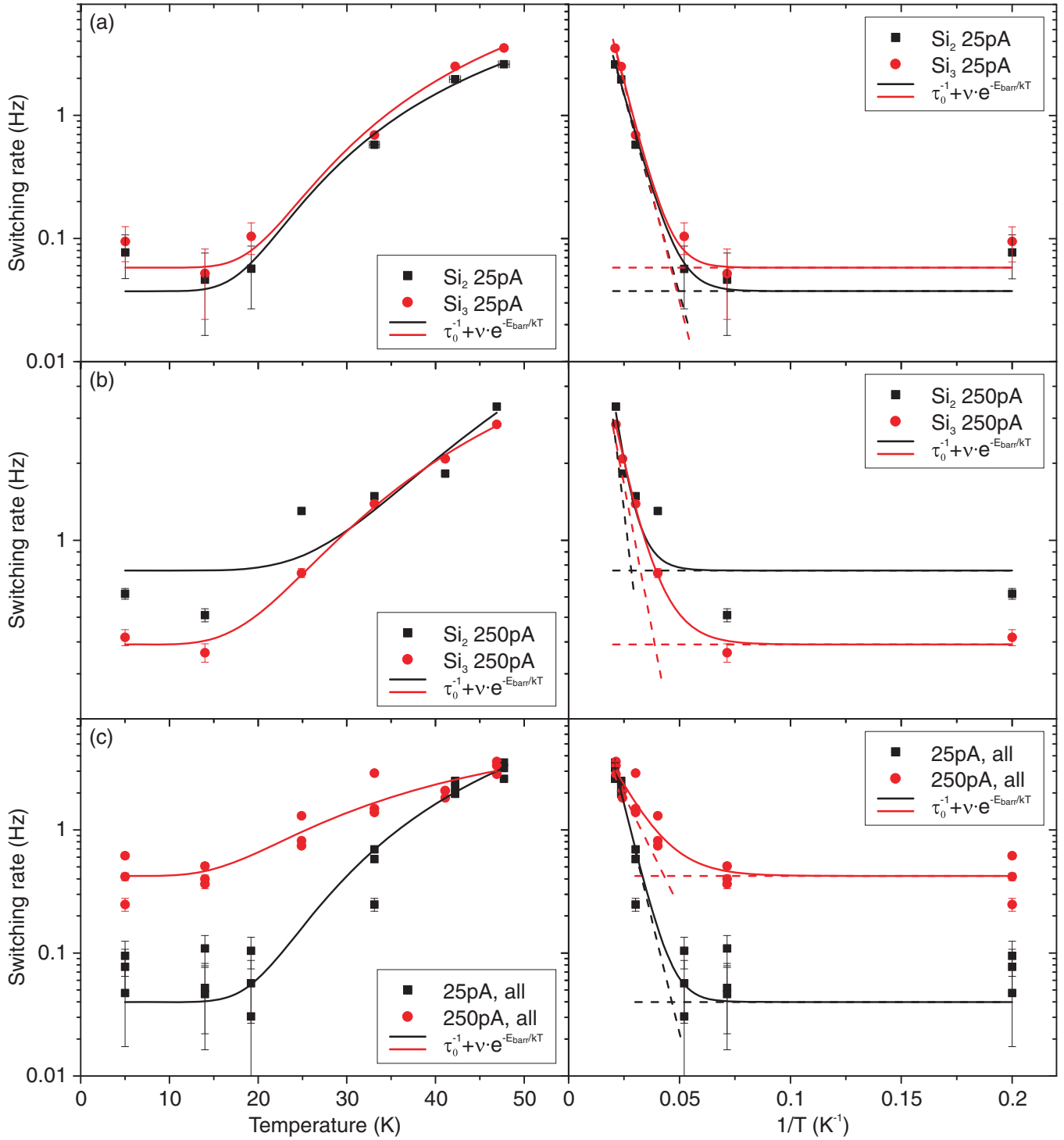


FIG. 8. (Color online) Switching rate τ^{-1} versus temperature T (left column) and versus $1/T$ (right column) for the individual donors at (a) 25 and (b) 250 pA and (c) for all three donors (c). The solid lines are fits with $\tau^{-1} = \tau_0^{-1} + \nu \cdot e^{-E_{\text{barr}}/kT}$. The contribution of the two terms is clear in the plots of τ^{-1} versus $1/T$.

of V_{crit} on the temperature indicates that switching takes place between metastable states. The constant switching rate below 20 K proves that a nonthermal process is involved, whereas the increasing switching rate with current suggests that inelastic tunneling processes are involved in switching the Si atom.

III. DISCUSSION

The model we propose to explain our observations is based on density functional theory (DFT) calculations of Si_{Ga} in the top layer of GaAs(110) (Ref. 20) and on the formation and dynamics of DX⁻ centers in bulk Si:GaAs (Refs. 27 and 28). Both bare a strong resemblance and can be related to the

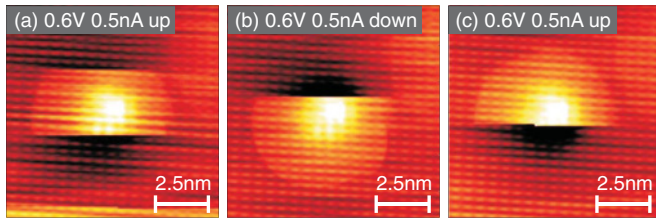


FIG. 9. (Color online) (a)–(c) Subsequent topography images on the same Si atom in the first layer of GaAs(110) measured at $V_{\text{crit}} = 0.6$ V at $T = 5$ K. Note the random position where the Si atom switches. Up and down refers to the slow scanning direction.

observed switching. DFT predicts a midgap state for Si atoms in the GaAs(110) surface ~ 0.5 eV below the conduction band. This calculation is only performed for the neutral situation, whereas the negatively charged situation might have a lower energy. This can be the case for the DX^- center in GaAs (Ref. 28), which is the second ingredient in our interpretation. This defect has been studied extensively for a number of donor species in different III-V semiconductor hosts. DX^- centers are donors that capture two electrons by relaxation to an interstitial position under hydrostatic pressure. In this configuration, a bond with a neighboring As atom is broken, creating two half-filled internal dangling bonds that are each saturated by a captured electron. These defects are deep states and are only stable when a second electron is bound to it (i.e., when they are negatively charged).

We propose the following model for our bistable Si atom, schematically shown in Fig. 10. We identify the white donor state as a configuration where the dangling bond is empty, which would be the case for the original Ga atom on the clean GaAs surface [Fig. 10(a)]. The empty bond is due to buckling,

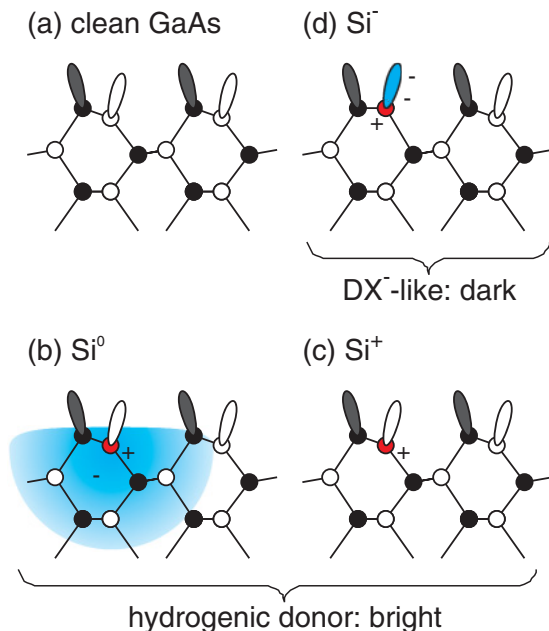


FIG. 10. (Color online) (a) A Ga atom on the clean GaAs surface has an empty dangling bond. (b,c) A surface Si atom with an empty dangling bond created a hydrogenic donor. (d) On the bare surface, the black Si^- configuration is favorable due to the saturated dangling bond. Red indicates the positive and blue the negative charge.

which is accompanied by a charge transfer between the Ga and the As atoms, resulting in an empty Ga dangling bond and a filled As dangling bond.^{29,30} Because Si replaces a Ga atom, an empty dangling bond can be expected, and in this configuration a shallow hydrogenic donor is created [Figs. 10(b) and 10(c)], which can be neutral or ionized. On the bare surface, where the dark state is favorable, we propose that the dangling bond is completely filled ($-2e$), thus the total charge is $-e$ [Fig. 10(d)]. This is similar to the DX^- center in bulk GaAs, which also has a filled dangling bond, and is only stable when negatively charged.

There are several indications that the tip can influence the lattice relaxation (i.e., induce a movement of the Si atom, and induce the switch). Previous STM experiments on GaAs(110) showed that the STM tip can influence buckling.³¹ The authors proposed that buckling is suppressed for small tip-sample distances, and a “truncated-bulk” situation is obtained (i.e., the surface atoms reside at their bulk positions, as expected for an unrelaxed surface). Furthermore, the DFT calculations in Ref. 20 show that the buckling is already reduced for a surface Si atom, compared to the clean GaAs surface.

Next we discuss the mechanism underlying the switching dynamics. Based on the fit to the experimental T dependence [Fig. 8], we conclude that the process is thermally activated for $T > 20$ K, but nonthermal processes dominate for $T < 20$ K. We explore quantum tunneling and inelastic processes as two possible nonthermal processes.

In the case of pure quantum tunneling, where the Si atom tunnels between two bonding configurations, no dependence on I_T is expected, whereas a constant ratio between τ^{-1} and I_T is expected for an inelastic process. The strong dependence of τ^{-1} on the tunneling current therefore points to an inelastic process. Note that the rate for both the transition from Si^- to $Si^{0/+}$ and the transition from $Si^{0/+}$ to Si^- depend on the tunnel current (i.e., both the excitation and the relaxation depend on I_T). Moreover, the Si atom switches when the tip is at random positions, not necessarily located close to the Si center. This holds especially for the $Si^{0/+}$ to Si^- transition. For an inelastic process, the transition preferentially occurs when the tip is located on top of the atom. However, in case of the excitation of phonons, which are less localized than the Si atom itself, this restriction is relaxed. Furthermore, the extended wave function of Si^0 [Fig. 10(b)] can facilitate a less localized excitation or relaxation.

Experimentally, we observe a high V_{crit} at low T , and a low V_{crit} at high T (see Fig. 7). We explain this as follows. We assume that the external voltage adjusts the relative positions of the potential minima corresponding to the $Si^{0/+}$ and the Si^- configurations, as is schematically shown in the insets in Fig. 7 and in more detail in Fig. 11. Rigidly shifting the curves with respect to each other affects the barrier height E_{barr} between the minima. We estimate that the voltage needed to align both parabolas is 0.2 V [Fig. 11(b)], based on the observation of $V_{\text{crit}} = 0.2$ V at 77 K. Below 0.2 V, Si^- is favorable [Fig. 11(a)], and above 0.2 V Si^+ is favorable [Figs. 11(c) and 11(d)]. In the range $0.2 \text{ V} < V < 1.0 \text{ V}$ the system is metastable; the white configuration is favorable, but the barrier between the minima is large. At high T , the large barrier can be crossed (thermally excited, similar to thermionic excitation over a Schottky barrier), and therefore the system goes to

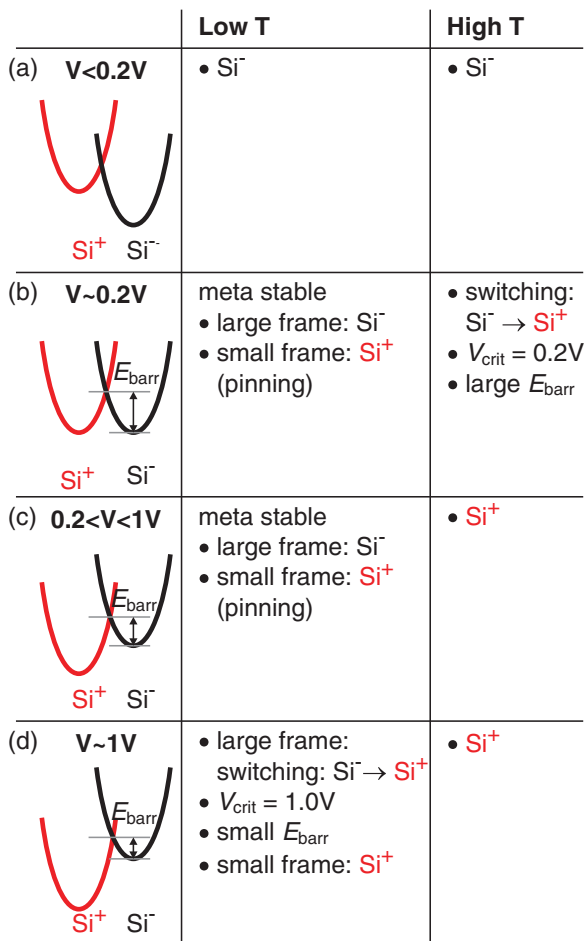


FIG. 11. (Color online) Schematic of our model. For $V < 0.2$ V, (a) the black Si^- configuration is favorable, (b,c) for 0.2 V $< V < 1.0$ V, the system is metastable for low T , and (d) for $V > 1.0$ V the white Si^+ configuration is favorable.

the Si^+ state as soon as the parabolas align at 0.2 V, thus $V_{\text{crit}} = 0.2$ V. At low T , however, the large barrier cannot be crossed thermally, and the system switches only when the barrier is sufficiently reduced by increasing the voltage to 1.0 V, thus $V_{\text{crit}} = 1.0$ V. This reduced barrier can either be crossed by quantum tunneling, or by inelastic excitations, or by a combination of both effects.

This concept of a metastable situation for 0.2 V $< V < 1.0$ V can furthermore explain the observed pinning at low T . At low T , the Si^- atom cannot cross the barrier up to 1 V, even though the donor-like configuration is favorable above 0.2 V. This is similar to the persistent photoconductivity at low temperatures observed for DX^- centers.²⁸ The region where the tip influences the energy landscape is of the order of the tip radius. For frame sizes larger than the tip radius, the potential landscape is modified only for a short period when the tip is located near the Si atom, and when the tip moves further along the scan line, the original potential landscape is restored, favoring and the black configuration. Therefore for large frame sizes, the black configuration is observed, even though the white configuration is favorable for short period in time. In case of scanning small frames, however, the tip is always close to the donor, giving the system sufficient time to

cross the large barrier. Once the Si atom has switched to $\text{Si}^{0/+}$, it will remain in this configuration.

The argumentation above leads to the following concept. Clearly inelastic processes are involved in the switching, which is proven by the dependence on the current setpoint, and possibly quantum tunneling is involved as well. The measured temperature dependence is very similar to the expected behavior for crossing a barrier with quantum tunneling. However, we cannot disentangle the contributions from inelastic processes and quantum tunneling. Based on the low attempt frequency, we propose a two-step process. DX^- centers in GaAs also follow a two-step process,^{28,32} where the DX^- center is first excited into a neutral DX^0 configuration, which is metastable. The DX^0 configuration can then either be further ionized into a substitutional donor configuration, or capture an electron from the CB and relax back into the DX^- configuration. Another example where a two-step process occurs, is the system of H atoms moving on Si(001) (Ref. 24). In this case, the barrier between two locations of the H atom is large. However, the system can be inelastically excited, which reduces the barrier significantly, and increases the tunnel probability through the remaining barrier. In our case, something similar could occur. The two-step process could be the subsequent capture of two electrons, similar to the DX^- center. Another possibility is that the system is inelastically excited, which reduces the remaining tunnel barrier (e.g., the excitation of a vibrational mode of the buckled surface atoms), which facilitates the geometrical motion of the Si atom by quantum tunneling. For all these two-step processes, we expect a low attempt frequency.

IV. CONCLUSION

We found that Si atoms in the surface layer of GaAs{110} switch between a donor-like $\text{Si}^{0/+}$ configuration and a negatively charged Si^- configuration at a critical voltage. Si^- is identified as a Si atom on an interstitial site similar to the DX^- center in bulk-GaAs. The bulk-like donor $\text{Si}^{0/+}$ is restored if the dangling bond at the Si site is depleted.

The switching rate depends on the feedback current and on the temperature. A constant switching rate below 20 K proves the existence of a nonthermal process. This process involves inelastic excitations, possibly in combination with quantum tunneling.

Our results emphasize the importance of the surface on the properties of dopants. In many studies, the impurities are described by their bulk properties. Typically the surface is only taken into account by assuming minor modifications. By now there are more and more indications of the significant impact of the surface, for example our own work on the enhanced binding energy¹⁵ and the switching discussed here. Also other groups report on the impact of the surface, for example Lee *et al.* reported that Mn atoms in the GaAs surface are insensitive to the TIBB, in contrast to subsurface impurities.³³

ACKNOWLEDGMENTS

We thank C. F. J. Flipse, S. Loth, P. A. Maksym, M. Rohlfing, M. Roy, M. Wenderoth, and L. Winking for helpful discussions, and the STW-VICI Grant No. 6631, COBRA, and NAMASTE for financial support.

*p.m.koenraad@tue.nl

- ¹Y. Cui, Q. Wei, H. Park, and C. M. Lieber, *Science* **293**, 1289 (2001).
- ²Ph. Ebert, *Surf. Sci. Rep.* **33**, 121 (1999).
- ³Z. F. Zhen, M. B. Salmeron, and E. R. Weber, *Appl. Phys. Lett.* **64**, 1836 (1994).
- ⁴Z. F. Zhen, M. B. Salmeron, and E. R. Weber, *Appl. Phys. Lett.* **65**, 790 (1994).
- ⁵G. Mahieu, B. Grandidier, D. Deresmes, J. P. Nys, D. Stiévenard, and Ph. Ebert, *Phys. Rev. Lett.* **94**, 26407 (2005).
- ⁶S. Loth, M. Wenderoth, L. Winking, R. G. Ulbrich, S. Malzer, and G. H. Döhler, *Phys. Rev. Lett.* **96**, 066403 (2006).
- ⁷A. M. Yakunin, A. Yu. Silov, P. M. Koenraad, J. H. Wolter, W. Van Roy, J. De Boeck, J.-M. Tang, and M. E. Flatté, *Phys. Rev. Lett.* **92**, 216806 (2004).
- ⁸D. Kitchen, A. Richardella, J.-M. Tang, M. E. Flatté, and A. Yazdani, *Nature (London)* **442**, 436 (2006).
- ⁹J. F. Zheng, X. Liu, N. Newman, E. R. Weber, D. F. Ogletree, and M. Salmeron, *Phys. Rev. Lett.* **72**, 1490 (1994).
- ¹⁰M. C. M. M. van der Wielen, A. J. A. van Roij, and H. van Kempen, *Phys. Rev. Lett.* **76**, 1075 (1996).
- ¹¹R. M. Feenstra, G. Meyer, F. Moresco, and K. H. Rieder, *Phys. Rev. B* **66**, 165204 (2002).
- ¹²C. Domke, Ph. Ebert, and K. Urban, *Surf. Sci.* **415**, 285 (1998).
- ¹³S. Loth, M. Wenderoth, K. Teichmann, and R. G. Ulbrich, *Solid State Commun.* **145**, 551 (2008).
- ¹⁴C. Celebi, J. K. Garleff, A. Yu. Silov, A. M. Yakunin, P. M. Koenraad, W. Van Roy, J.-M. Tang, and M. E. Flatté, *Phys. Rev. Lett.* **104**, 086404 (2010).
- ¹⁵A. P. Wijnheijmer, J. K. Garleff, K. Teichmann, M. Wenderoth, S. Loth, R. G. Ulbrich, P. Maksym, M. Roy, and P. M. Koenraad, *Phys. Rev. Lett.* **102**, 166101 (2009).
- ¹⁶J. K. Garleff, A. P. Wijnheijmer, A. Yu. Silov, J. van Bree, W. Van Roy, J.-M. Tang, M. E. Flatté, and P. M. Koenraad, *Phys. Rev. B* **82**, 035303 (2010).
- ¹⁷T. O. Strandberg, C. M. Canali, and A. H. MacDonald, *Phys. Rev. B* **80**, 024425 (2009).
- ¹⁸J. K. Garleff, M. Wenderoth, K. Sauthoff, R. G. Ulbrich, and M. Rohlfing, *Phys. Rev. B* **70**, 245424 (2004).
- ¹⁹R. M. Feenstra, J. M. Woodall, and G. D. Pettit, *Phys. Rev. Lett.* **71**, 1176 (1993).
- ²⁰J. Wang, T. A. Arias, J. D. Joannopoulos, G. W. Turner, and O. L. Alerhand, *Phys. Rev. B* **47**, 10326 (1993).
- ²¹K. Teichmann, M. Wenderoth, S. Loth, R. G. Ulbrich, J. K. Garleff, A. P. Wijnheijmer, and P. M. Koenraad, *Phys. Rev. Lett.* **101**, 076103 (2008).
- ²²A. P. Wijnheijmer, J. K. Garleff, K. Teichmann, M. Wenderoth, S. Loth, R. G. Ulbrich, and P. M. Koenraad, (unpublished).
- ²³M. Sakurai, C. Thirstup, and M. Aono, *Appl. Phys. A* **80**, 1153 (2005).
- ²⁴K. Stokbro, U. J. Quaade, R. Lin, C. Thirstup, and F. Grey, *Faraday Discuss.* **117**, 231 (2000).
- ²⁵A. Saedi, A. v. Houselt, R. v. Gastel, B. Polsema, and J. W. Zandvliet, *Nano Lett.* **5**, 1733 (2009).
- ²⁶A. J. Heinrich, C. P. Lutz, J. A. Gupta, and D. M. Eigler, *Science* **298**, 1381 (2002).
- ²⁷D. J. Chadi and K. J. Chang, *Phys. Rev. Lett.* **61**, 873 (1988).
- ²⁸P. M. Mooney, *Semicond. Sci. Technol.* **6**, B1 (1991).
- ²⁹J. R. Chelikowsky and M. L. Cohen, *Solid State Commun.* **29**, 267 (1979).
- ³⁰J. R. Chelikowsky and M. L. Cohen, *Phys. Rev. B* **20**, 4150 (1979).
- ³¹G. J. de Raad, D. M. Bruls, P. M. Koenraad, and J. H. Wolter, *Phys. Rev. B* **64**, 075314 (2001).
- ³²L. Dobaczewski and P. Kaczor, *Phys. Rev. Lett.* **66**, 68 (1991).
- ³³D. H. Lee and J. A. Gupta, *Science* **330**, 1807 (2010).